1990SoPh..126..319P

MAGNETIC FIELD EVOLUTION DURING PROMINENCE ERUPTIONS AND TWO-RIBBON FLARES

E. R. PRIEST* and T. G. FORBES

Space Science Center, Science Engineering Research Building, Durham, NH 03824, U.S.A.

(Received 15 June, 1989; in revised form 17 November, 1989)

Abstract. Simple models for the MHD eruption of a solar prominence are presented, in which the prominence is treated as a twisted magnetic flux tube that is being repelled from the solar surface by magnetic pressure forces. The effects of different physical assumptions to deal with this magneto-hydrodynamically complex phenomenon are evaluated, such as holding constant the prominence current, radius, flux or twist or modelling the prominence as a current sheet. Including a background magnetic field allows the prominence to be in equilibrium initially with an Inverse Polarity and then to erupt due to magnetic non-equilibrium when the background magnetic field is too small or the prominence twist is too great. The electric field at the neutral point below the prominence rapidly increases to a maximum value and then declines. Including the effect of gravity also allows an equilibrium with Normal Polarity to exist. Finally, an ideal MHD solution is found which incorporates self-consistently a current sheet below the prominence and which implies that a prominence will still erupt and form a current sheet even if no reconnection occurs. When reconnection is allowed it is, therefore, driven by the eruption.

Introduction

Eruptions of solar prominences are thought to be caused by an instability or lack of equilibrium in a magnetic arcade. This may occur when the magnetic field is twisted or sheared too much or the prominence altitude becomes too great or the feet become too far apart (Van Tend and Kuperus, 1978; Sturrock, 1980; Hood and Priest, 1980; Browning and Priest, 1986; Zwingmann, 1985; Amari and Aly, 1989; Demoulin and Priest, 1988). The eruption is expected to drive reconnection and heating in a current sheet that forms about an X-type neutral point below the rising prominence (Priest, 1981; Steele and Priest, 1989). Detailed numerical experiments of reconnection in such a sheet have been investigated (Forbes and Priest, 1983; Robertson and Priest, 1987) and global numerical models have recently been set up (Mikic, Barnes, and Schnack, 1988; Biskamp and Welter, 1989).

The aim of the present paper is to study magnetic field evolution (including reconnection and the creation of current sheets) below erupting prominences, both quiescent and active-region, by means of a complementary simple analytical model which elucidates some of the physics in this complex process. The prominence is generally modelled as a flux tube (or line current) above the photosphere in the same way as Van Tend and Kuperus (1978), who found non-equilibrium when the prominence height is too great; their work has been put on a firm mathematical foundation and extended by Amari and Aly (1989) and Demoulin and Priest (1988), who have elucidated the

* Permanent address: Mathematical Sciences Dept., North Haugh, St Andrews, KY16 9SS, Scotland.

Solar Physics **126:** 319–350, 1990.
© 1990 *Kluwer Academic Publishers. Printed in Belgium.*

© Kluwer Academic Publishers • Provided by the NASA Astrophysics Data System

1990SoPh..126..319P

conditions for non-equilibrium. Line tying by the dense photosphere is simulated by including an image flux tube (Kuperus and Raadu, 1974), but circuit equations are not employed (Kaastra, 1985; Kuin and Martens, 1986; Martens, 1986) since we do not believe that they give an adequate modelling of the MHD of the process (Priest, 1986).

In Section 2 we begin with the simplest model of an erupting prominence, namely a straight horizontal flux tube which is moving upwards due to the repulsion from an image flux tube. The effects of different assumptions are evaluated, such as holding the prominence current and radius constant or of instead keeping the prominence flux or twist constant. Also modelling the prominence as a current sheet rather than a flux tube is considered. In Section 3 the effects of a background active region field and of gravity are included so that the prominence can be initially in equilibrium and then erupt due to non-equilibrium or instability. Finally, in Section 4 the additional complication of including a reconnecting current sheet below the prominence is evaluated.

2. Simple Prominence

In order to elucidate some of the basic properties of an erupting prominence we first of all consider the simplest model namely that of a straight horizontal flux tube (or line current $2\pi I/\mu$) whose axis H is located a distance h above an origin O in a line-tying surface (the photosphere). The effect of line tying is taken into account by placing an image flux tube (with current $-2\pi I/\mu$) at a distance h below the photosphere (the x-axis) as shown in Figure 1(a). The resulting magnetic field may be written most elegantly in terms of the complex variable $z = x + iy$ as

$$B_y + iB_x = \frac{I}{z - ih} - \frac{I}{z + ih} = \frac{2ihI}{z^2 + h^2} \,. \tag{1}$$

Note that regarding $2\pi I/\mu$ as the current rather than I removes the factor of $\mu/(2\pi)$ that normally appears in Equation (1) in MKS units.

It should be noted that, although in a vacuum one may switch on a current in a wire and produce a magnetic field of the above form outside the wire, the same physics does not apply in the solar atmosphere. Here currents are not driven by electric fields but instead arise in a secondary manner from force balance and magnetic field evolution (e.g., Priest, 1982, 1986). For example, as one twists up a flux tube through motions of its footpoints, one may increase the current and azimuthal field locally. The magnetic field around the line currents in Figure 1 should not be thought of as being produced by the current, but represents instead a simple model of the ambient magnetic field in which the flux tube is located: more realistic models will be proposed in the following sections.

The magnetic field of Equation (1) refers to the field outside the prominence and, in view of the singularities at $z = \pm ih$, we shall cut it off at some distance R_p from the singularities. Furthermore, in the case when $R_p \ll h$ we shall assume that R_p is independent of the angular direction from H, so that the cut-off curve is approximately a

© Kluwer Academic Publishers • Provided by the NASA Astrophysics Data System

1990SoPh..126..319P

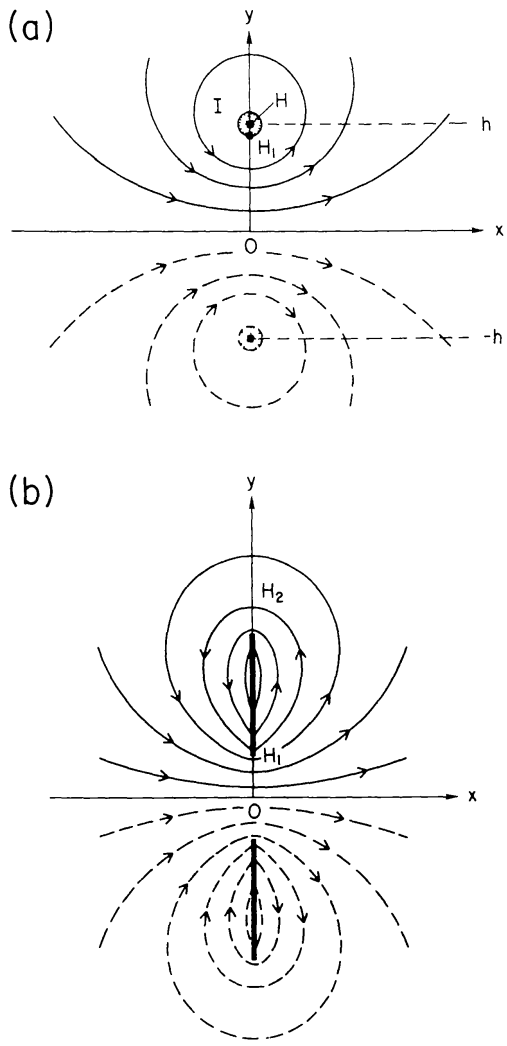

Fig. 1. The notation for a section through an isolated prominence with continuous magnetic field lines and repelled by an image prominence having dashed field lines. The prominence is modelled as (a) a flux tube with current I at a point H a distance h above the photosphere or (b) a vertical current sheet stretching from H_1 to H_2.

circle. Inside the flux tube we shall assume a purely azimuthal field

$$B_i = B_p \frac{r}{R_p} , \tag{2}$$

where B_p ($\approx I/R_p$) is the field at the surface of the flux tube (or prominence).

Now the vertical equation of motion of the flux tube (of mass M) moving under the repulsion from the image alone (a distance $2h$ away) is

$$\frac{\mathrm{d}}{\mathrm{d}t}\left(M\frac{\mathrm{d}h}{\mathrm{d}t}\right) = F \equiv \frac{\pi I^2}{\mu h} . \tag{3}$$

Also the magnetic flux ψ_O crossing the y-axis below the flux tube between O and H_1

© Kluwer Academic Publishers • Provided by the NASA Astrophysics Data System

1990SoPh..126..319P

(the point where the lower part of the flux tube intersects the y-axis, Figure 1(a)) is

$$\psi_O = \int_0^{h-R_P} B_x(0, y)\, \mathrm{d}y$$

or

$$\psi_O = I \log\left(\frac{2h}{R_P} - 1\right). \tag{4}$$

If the flux tube starts from rest at a height h_0, its subsequent speed upwards ($v = \mathrm{d}h/\mathrm{d}t$) may be found by integrating (3) to give

$$\frac{1}{2} M v^2 = \int_{h_0}^{h} \frac{\pi I^2}{\mu h}\, \mathrm{d}h\,, \tag{5}$$

where the term on the right-hand side is minus the potential energy or the work done by the force of repulsion.

Since (3) determines $h(t)$ in terms of $I(t)$ we need to make an assumption to determine I and there are several possibilities, as enumerated below and sketched in Figure 2.

2.1. Constant current (I)

This may seem (at first) an attractively simple assumption which leads to a speed of rise increasing in an unbounded manner (Figure 2) like

$$v^2 = \frac{2\pi I^2}{\mu M} \log \frac{h}{h_0}\,. \tag{6}$$

However, the magnetic energy in the system (outside the flux tubes) is

$$W_B = \int\int \frac{2h^2 I^2/\mu}{[x^2 + (y-h)^2][x^2 + (y+h)^2]}\, \mathrm{d}x\, \mathrm{d}y\,, \tag{7}$$

where circles of radius R_P about $z = \pm ih$ are excluded. For $h \gg R_P$ and I constant it becomes

$$W_B \approx \frac{\pi I^2}{\mu} \log \frac{h}{R_p}\,, \tag{8}$$

which surprisingly increases with h (for constant R_P), whereas, since the repulsive force does work as the flux tube moves up, one would have expected the magnetic potential energy to decrease! Indeed, the work done by the repulsive force is

$$W = -\int_{h_0}^{h} \frac{\pi I^2}{\mu h}\, \mathrm{d}h = -\frac{\pi I^2}{\mu} \log \frac{h}{h_0}\,.$$

© Kluwer Academic Publishers • Provided by the NASA Astrophysics Data System

1990SoPh..126..319P

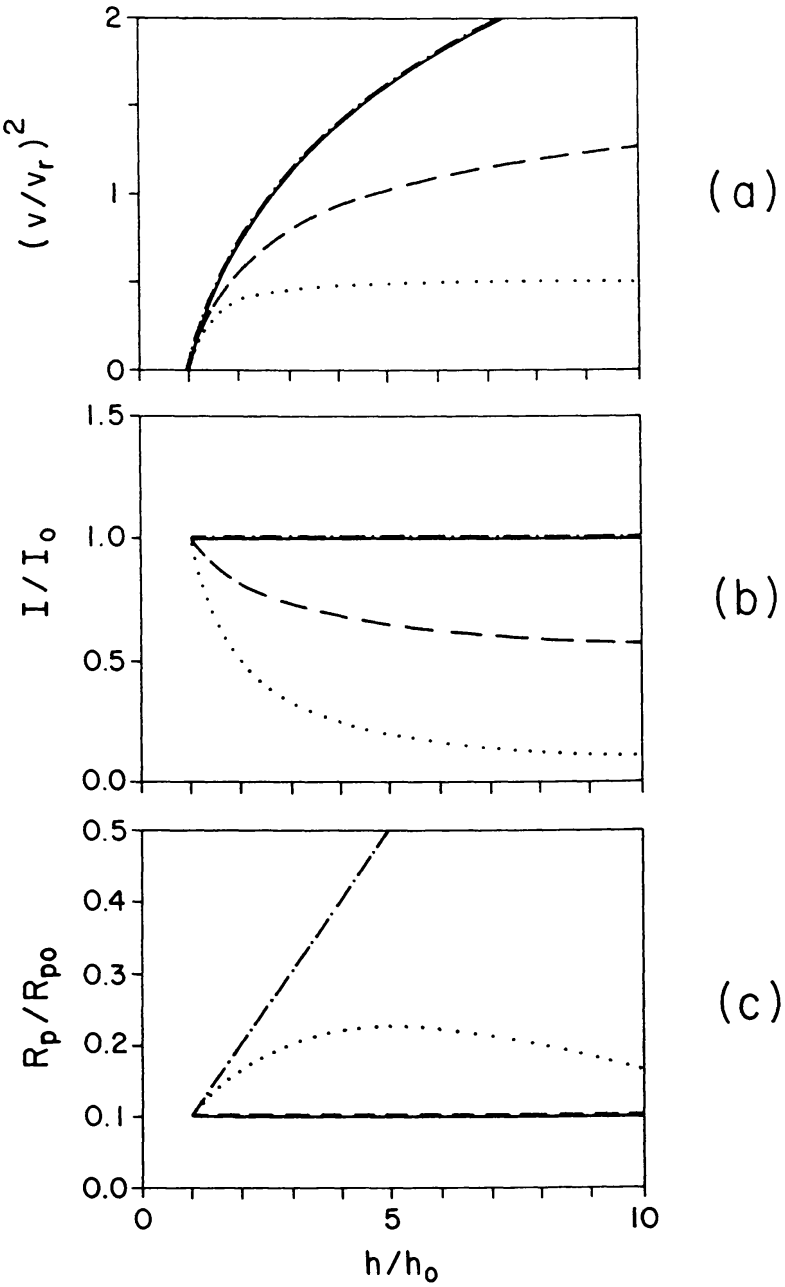

Fig. 2. The rise speed (v), current (I) and flux tube radius (R_p) for: a constant current (_____), a constant flux tube radius (_ _ _ _ _), constant twist (. . . . . .), and constant magnetic fluxes (_ . _ . _ . _). The rise speed is measured in units of a typical speed $v_r = (\pi/\mu M)^{1/2} I_0$.

The resolution of this paradox is that the magnetic flux $2\psi_O$ (from (4)) through a circuit consisting of the current I, its image $-I$ and their closure at infinity is increasing in time and so the current sources at infinity are also doing work. Consequently, this case is not the most realistic.

2.2. Constant flux tube radius (R_P)

If we assume the flux ψ_O remains constant, Equation (4) determines I provided we know how R_P varies. If, for example, the flux tube is modelled as a rigid structure of constant

© Kluwer Academic Publishers • Provided by the NASA Astrophysics Data System

1990SoPh..126..319P

radius (R_P), then, as shown in Figure 2, the current decreases as

$$I = \frac{\psi_O}{\log(2h/R_P - 1)} = \frac{I_0 \log(2h_0/R_P - 1)}{\log(2h/R_P - 1)} ,$$

and for $R_P \ll h_0$ the rise speed from (5) increases with height like

$$v^2 = \frac{\pi\psi_O^2}{\mu M}\left(\frac{1}{\log(2h_0/R_P - 1)} - \frac{1}{\log(2h/R_P - 1)}\right) , \tag{9}$$

approaching a constant value at large altitudes of

$$v_\infty^2 = \frac{\pi\psi_O^2}{\mu M \log(2h_0/R_P - 1)} = \frac{\pi I_0^2}{\mu M}\log\left(\frac{2h_0}{R_P} - 1\right) . \tag{10}$$

Correspondingly, the work done by the repulsive force is

$$W = \frac{\pi I_0^2}{\mu}\left(\log\frac{2h_0}{R_P}\right)^2\left(\frac{1}{\log 2h/R_P} - \frac{1}{\log 2h_0/R_P}\right) .$$

If it is assumed that the field (B_i) within the filament matches continuously to the external magnetic field, then constant R_P implies that the magnetic flux (ψ_P) in the tube decreases with height, i.e.,

$$\psi_P = \int_0^{R_P} B_i \, dr = \frac{1}{2} R_P B_P = \frac{Ih}{2h - R_p} \approx \frac{1}{2} I . \tag{11}$$

However, if there is a surface current on the filament, the B_i need not match continuously to the external magnetic field and consequently ψ_P would not necessarily increase with height.

2.3. Constant Magnetic Fluxes

Another possibility is to hold fixed the fluxes ψ_O and ψ_P, both between the photosphere and the prominence and also inside the prominence. For $h \gg R_P$, we then have (Figure 2)

$$B_P \approx \frac{I}{R_P}, \qquad \psi_O \approx I \log\frac{2h}{R_P}, \qquad \psi_P \approx \frac{1}{2} I ,$$

so that I remains constant, while the tube radius increases linearly with height,

$$R_P \approx 2h \exp\left(-\frac{\psi_O}{2\psi_P}\right) , \tag{12}$$

and the prominence field decreases with height,

$$B_P \approx \frac{2\psi_P}{h} \exp\left(-\frac{\psi_O}{2\psi_P}\right) . \tag{13}$$

© Kluwer Academic Publishers • Provided by the NASA Astrophysics Data System

1990SoPh..126..319P

In this case the speed of rise increases indefinitely (Equation (6)) and the magnetic energy W_B (Equation (8)) remains constant. In a two-dimensional, coplanar numerical experiment Forbes (1990) found that ψ_O and ψ_P are indeed nearly constant when the magnetic Reynolds number of the system is very large. However, R_P does not increase as fast as predicted by (12) and consequently a surface current appears on the filament. Thus, in general the filament properties in this numerical experiment are more nearly like those of Section 2.2.

2.4. Constant twist

For a rising magnetic three-dimensional flux tube there is no clear reason why ψ_P should remain constant since the tube may locally untwist or twist up and so decrease or increase the field in the plane of Figure 1. If the ends of the flux tube are anchored down in the solar surface a good approximation is to regard the net twist Φ along the tube as being constant. If its length is L, then in terms of the axial field (B_z) and the azimuthal field (B_P) the surface twist may be written approximately as

$$\Phi = \frac{LB_P}{R_P B_z} \approx \frac{LI}{R_P^2 B_z} \,. \tag{14}$$

For a uniform axial field (B_z), the constancy of axial flux then implies that $R_P^2 B_z$ is constant and so, by assuming that L increases roughly linearly with h (Steele and Priest, 1989), we obtain that hl remains constant or

$$I = I_0 \frac{h_0}{h} \tag{15}$$

in terms of the initial current (I_0) and height (h_0).

In this case Equation (4) determines the tube radius to be approximately

$$R_P = 2h \exp\left(- \frac{\psi_{OP} h}{I_0 h_0} \right) ,$$

which increases to a maximum value of $(2I_0 h_0/(\psi_{OP} e))$ at $h = I_0 h_0/\psi_{OP}$ and thereafter declines to zero as h approaches infinity (Figure 2). At the same time the rise speed from (5) is given by

$$v^2 = \frac{\pi I_0^2 h_0^2}{\mu M} \left(\frac{1}{h_0^2} - \frac{1}{h^2} \right) \tag{16}$$

and so increases monotonically to a value $(\pi/\mu M)^{1/2} I_0$ at large altitudes.

2.5. Bennett's relation

Although the net upwards force on the flux tube arises from the global effect of the surrounding magnetic field and the small departure of the flux tube from a circular shape, the local magnetic equilibrium of the flux tube (neglecting that departure) gives rise to

© Kluwer Academic Publishers • Provided by the NASA Astrophysics Data System

1990SoPh..126..319P

a constraint known as Bennett's relation. Thus, if the field component out of the plane of Figure 1 is uniform, the local radial force balance is

$$\frac{\mathrm{d}}{\mathrm{d}r}\left(p_i + \frac{B_i^2}{2\mu}\right) + \frac{B_i^2}{\mu r} = 0\,,$$

which, after using (2), determines the internal pressure to be

$$p_i = p_e + \frac{I^2}{\mu R_P^4}(R_P^2 - r^2)\,. \tag{17}$$

Here p_e is the external pressure, which for the external potential field of Equation (1) we shall neglect by comparison with the magnetic pressure. Now the mass (per unit length) of the flux tube is

$$M = \int_0^{R_P} \rho_i\, 2\pi r\, \mathrm{d}r\,,$$

and so for a uniform temperature T and a gas law $p_i = R\rho_i T$ this gives the Bennett relation

$$M = \frac{\pi I^2}{2\pi\mu R T}\,. \tag{18}$$

Thus, if the mass and temperature remain constant, we recover the constant current case (i), but in general they both may change in time in a prescribed way. For example the prominence temperature may rise as it is heated up or cool adiabatically as it expands. Furthermore, the mass may decrease as plasma flows down along the flux tube to the solar surface or it may increase as extra mass is entrained.

2.6. Prominence as a Current Sheet

We may instead follow Demoulin and Priest (1990) in modelling the prominence as a small current sheet of length l (Figure 1(b)) stretching vertically between points H_1 and H_2 at altitudes $h - l/2$ and $h + l/2$, respectively. The flux function for a single line current $(\mu I/2\pi)$ at a height h together with its image $(-\mu I/2\pi)$ at height $-h$ is

$$A = IG\,,$$

where

$$G(z, h) = -\log\frac{z - ih}{z + ih} \tag{19}$$

is the Green's function. Thus if the current density at height h' in the current sheet is $\mu j(h')/2\pi$, the flux function for the current sheet may be written

$$A = \int_{h-l/2}^{h+l/2} j(h')G(z, h')\,\mathrm{d}h'\,. \tag{20}$$

© Kluwer Academic Publishers • Provided by the NASA Astrophysics Data System

1990SoPh..126..319P

In particular, the value on the y-axis is

$$A(0, y) = \int_{h-l/2}^{h+l/2} j(h') \log \left| \frac{y - h'}{y + h'} \right| \mathrm{d}h' \tag{21}$$

At the point H_1 this becomes for a uniform current density ($j(h')l = I$)

$$\psi_O = \left(\log \frac{l}{2h - l} - \frac{2h}{l} \log \frac{2h}{2h - l} \right) ,$$

or, for $2h \gg l$,

$$\psi_O \approx I \left(1 + \log \frac{2h}{l} \right) . \tag{22}$$

Thus for constant ψ_O and l, the current falls off with height as

$$I = \frac{I_0(1 + \log 2h_0/l)}{1 + \log 2h/l} , \tag{23}$$

while from (5) the rise speed is given by

$$v^2 = \frac{2\pi\psi_O}{\mu M} \left(\frac{1}{1 + \log 2h_0/l} - \frac{1}{1 + \log 2h/l} \right) , \tag{24}$$

which approaches a constant value of $2\pi I_0^2/(\mu M(1 + \log 2h_0/l))$ at large heights (Figure 2). Modelling the prominence as a current sheet is an improvement on treating it as a line current since it is observed to be tall and thin. The solution above (20) lays the foundations for an improved model, although by itself it suffers from the self-pinching problem identified by Anzer (1989) in relation to the Kuperus–Raadu model. However, such a difficulty disappears when a sufficiently large ambient field is superimposed (as in Section 3.6).

3. Prominence in a Background Field

3.1. Depressed dipole – Inverse Polarity Solutions

Next let us suppose the prominence is supported in a background magnetic field due to, for example (but not necessarily), an active region and modelled by a dipole of moment m (a distance h_b below the photosphere, Figure 3), so that

$$B_y + iB_x = \frac{I}{z - ih} - \frac{I}{z + ih} + \frac{im}{(z + ih_b)^2} . \tag{25}$$

The image at $z = -ih$ ensures that the normal field on the photosphere ($y = 0$) is independent of I and h.

© Kluwer Academic Publishers • Provided by the NASA Astrophysics Data System

1990SoPh..126..319P

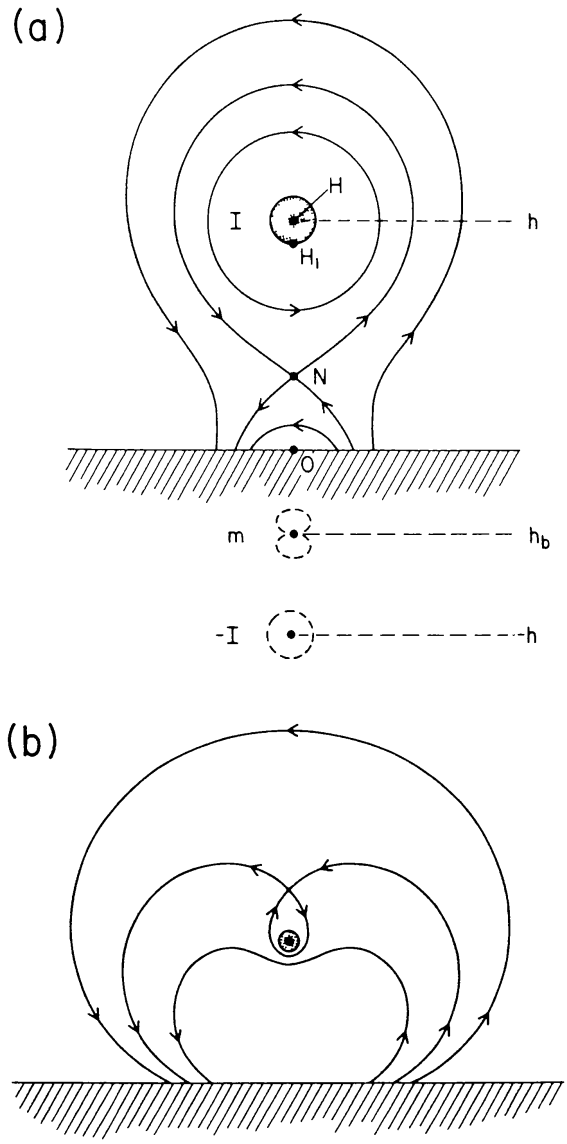

Fig. 3. The notation for a section through a prominence in a background field and with (a) inverse polarity; (b) normal polarity.

Neutral points are located at points $z = iy_N$ on the y-axis such that

$$y_N^2\left(1 + \frac{2hI}{m}\right) + \frac{4hI}{m} h_b y_N - \left(h^2 - \frac{2hI}{m} h_b^2\right) = 0\,, \tag{26}$$

and so the values of y_N/h_b depend on h_bI/m and h/h_b. In particular, a neutral point appears above the solar surface ($y = 0$) when $h/h_b > 2Ih_b/m$. When $h_bI/m \ll 1$, the upper neutral point becomes approximately

$$y_N = \frac{h}{a}\left(1 - \frac{h_bI}{m}\left(\frac{h_b}{h} + \frac{2}{a}\right)\right)\,,$$

where $a^2 = (1 + 2hI/m)$.

© Kluwer Academic Publishers • Provided by the NASA Astrophysics Data System

1990SoPh..126..319P

The vertical equation of motion becomes

$$\frac{\mathrm{d}}{\mathrm{d}t}\left(M\frac{\mathrm{d}h}{\mathrm{d}t}\right) = F \equiv \frac{2\pi I}{\mu}\left(\frac{I}{2h} - \frac{m}{(h+h_b)^2}\right) . \tag{27}$$

Equilibrium occurs for a given I and h_b when the filament height (h) is given by

$$\frac{h}{h_b} = \left(\frac{m}{h_b I} - 1\right) \pm \left(\frac{m}{h_b I}\left(\frac{m}{h_b I} - 2\right)\right)^{1/2} , \tag{28}$$

which gives two solutions when $m/(h_b I) > 2$ and no solutions when $m/(h_b I) < 2$ (Figure 4(a)). When $h_b I/m \ll 1$, the equilibrium becomes approximately

$$h = \frac{2m}{I}\left(1 - \frac{h_b I}{m}\right) .$$

At the non-equilibrium point $h = h_b$ and there is one solution. The lower branch is stable and the upper branch is unstable in such a way that to the left of the non-equilibrium

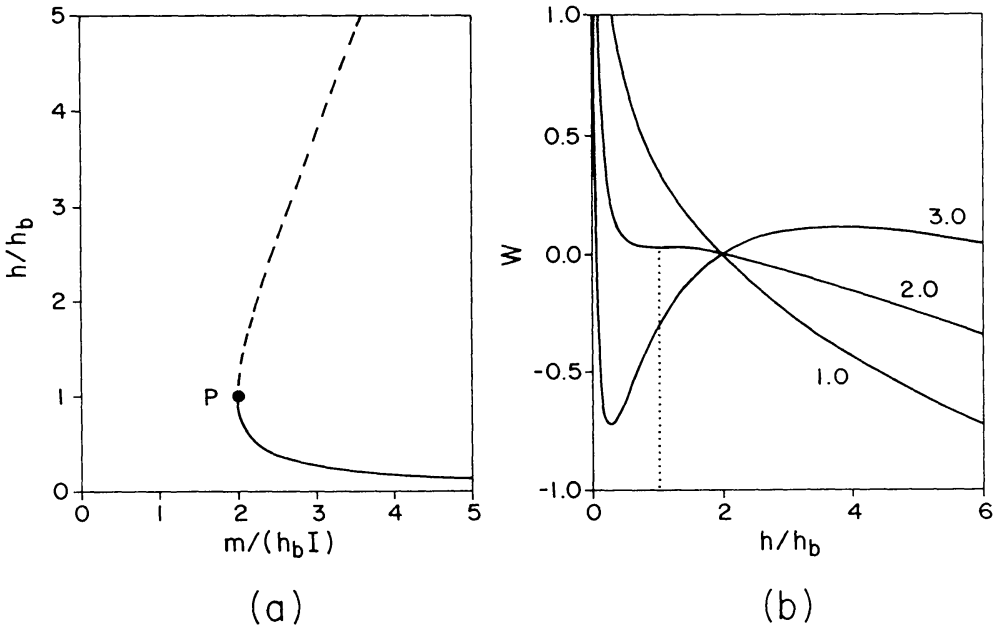

Fig. 4. (a) The equilibrium prominence height (h) as a function of m/I, where m is the background dipole strength and I the prominence current. The continuous equilibrium is stable and the dashed one unstable. P is a non-equilibrium point. (b) The potential energy W (in units of $\pi I^2/\mu$) as a function of prominence height h for values of $m/(h_b I)$ equal to 1, 2, and 3. The dotted line indicates the location corresponding to point P in Figure 4(a).

point or above the unstable branch the unbalanced force is upwards and so causes the filament to erupt. This can also be seen from the potential energy curve $W(h)$ in Figure 4(b) which arises from integrating the force given in (27):

$$W = -\int_{h_0}^{h} F\,\mathrm{d}h = -\frac{2\pi I}{\mu}\left(\frac{I}{2}\log\frac{h}{h_0} + \frac{m(h_0 - h)}{(h+h_b)(h_0+h_b)}\right) . \tag{29}$$

© Kluwer Academic Publishers • Provided by the NASA Astrophysics Data System

1990SoPh..126..319P

Thus as the dipole moment (m) decreases or the dipole depth (h_b)increases or the flux tube current (I) increases, so the prominence passes through a series of gradually increasing equilibrium heights until when $m/(h_b I)$ becomes less than 2 there is no longer an equilibrium and the prominence erupts.

If the flux tube starts from rest at height h_0, its subsequent rise speed ($v = \mathrm{d}h/\mathrm{d}t$) is given from (27) by

$$\frac{1}{2} M v^2 = \int_{h_0}^{h} \frac{\pi I^2}{\mu h} - \frac{2\pi I m/\mu}{(h + h_b)^2} \, \mathrm{d}h \,. \tag{30}$$

In particular if I and m remain constant we find

$$v^2 = \frac{2\pi I^2}{\mu M} \left(\log \frac{h}{h_0} + \frac{2m(h_0 - h)}{I(h + h_b)(h_0 + h_b)} \right) .$$

Thus when I is positive the effect of the ambient magnetic field trying to pull down the flux tube slows down the rise, since the second term on the right-hand side is negative, although the rise speed still increases indefinitely (Figure 5).

The magnetic flux between the photosphere and the neutral point below the prominence is

$$\psi_{ON} = \int_0^{y_N} B_x(0, y) \, \mathrm{d}y = I \log \frac{h + y_N}{h - y_N} - \frac{m y_N}{(y_N + h_b) h_b} \,,$$

or, when $h_b I/m \ll 1$ and $h_b \ll y_N$,

$$\psi_{ON} = I \log \frac{(1 + 2hI/m)^{1/2} + 1}{(1 + 2hI/m)^{1/2} - 1} - \frac{m}{h_b} \,. \tag{31}$$

At large heights $h \gg m/I$ this reduces to

$$\psi_{ON} = \left(\frac{2Im}{h} \right)^{1/2} - \frac{m}{h_b} \,.$$

As the prominence rises so the magnetic field in general reconnects at the neutral point N and the flux ψ_{ON} increases (although the net flux ψ_O remains constant (Section 3.4)). The resulting electric field is (assuming m remains constant)

$$E_N = \frac{\partial \psi_{ON}}{\partial t} = \frac{\mathrm{d}I}{\mathrm{d}t} \log \frac{(1 + 2hI/m)^{1/2} + 1}{(1 + 2hI/m)^{1/2} - 1} - \frac{1}{h} \left(1 + \frac{2hI}{m} \right)^{-1/2} \frac{\mathrm{d}}{\mathrm{d}t} (hI) \,, \tag{32}$$

or, at large heights $h \gg m/I$,

$$E_N = \left(\frac{mh}{2I} \right)^{1/2} \frac{\mathrm{d}}{\mathrm{d}t} \left(\frac{I}{h} \right) .$$

© Kluwer Academic Publishers • Provided by the NASA Astrophysics Data System

1990SoPh..126..319P

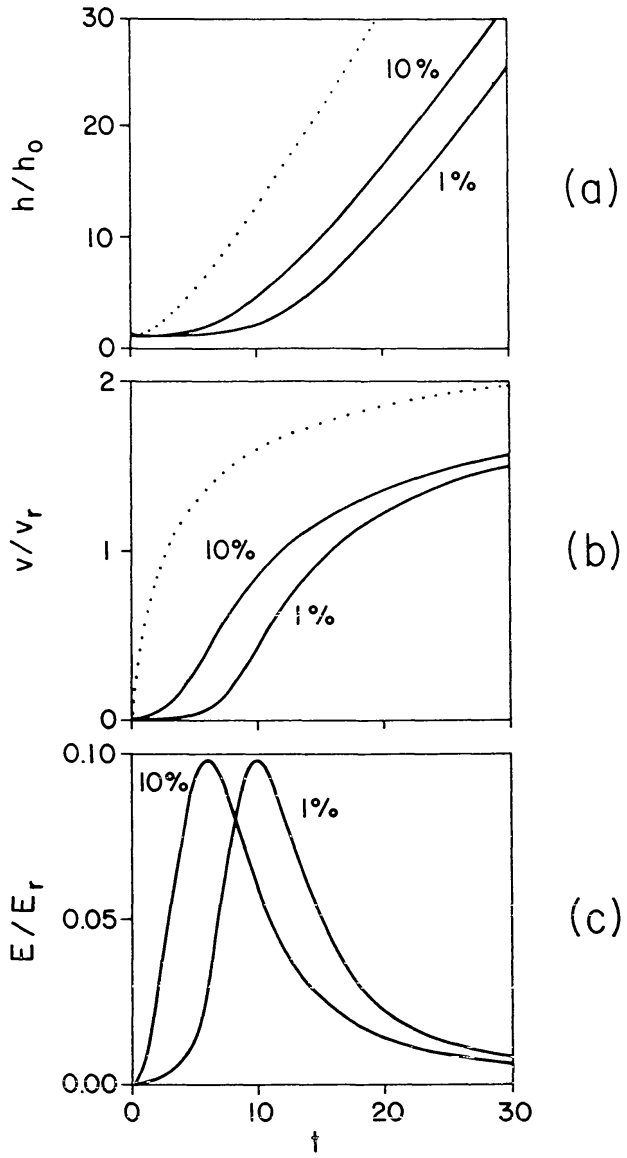

Fig. 5. The prominence height (h), rise speed (v), and neutral point electric field (E_r) as functions of time (in units of h_0/v_r) for constant filament current. The dotted curve is the case with no background field ($m = 0$), while the solid curves are those with a background field ($m = 1$) and with a 1% and a 10% perturbation of the filament in the upwards direction from its equilibrium position.

Thus in the particular case when I remains constant

$$E_N = -\left(\frac{mI}{2}\right)^{1/2} \frac{v}{h^{3/2}} ,$$

where $v = \mathrm{d}h/\mathrm{d}t$. Figure 5(c) plots the electric field at the X-line as a function of time for the constant filament current model with $h_b = 0$. The electric field peaks when the filament height (h) equals $\exp 0.5$, i.e., $h = 1.65$, and the value of the electric field at this peak is independent of the initial perturbation as long as the perturbation is small.

The variation of the electric field shown in Figure 5(c) is qualitatively very similar to that inferred by Poletto and Kopp (1986) from the time behaviour of the chromospheric

© Kluwer Academic Publishers • Provided by the NASA Astrophysics Data System

1990SoPh..126..319P

ribbons produced by the large flares of 29 July, 1973 and 21 May, 1980. In these flares the electric field increased rapidly to a peak value about 20 to 30 min after flare onset, and then it decreased at a slower rate over a period of several hours in a manner reminiscent of Figure 5(c). In terms of the present model, this behaviour occurs because the flare's electric field is determined entirely by the dynamics of the filament motion if reconnection is allowed to proceed as rapidly as needed.

3.2. Background Dipole Close to Photosphere

When the prominence height (h) is much larger than the depth (h_b) of the background, the magnetic field becomes

$$B_y + iB_x = \frac{i(2hI + m)(z^2 - z_N^2)}{(z^2 + h^2)z^2}\,, \tag{33}$$

where $z_N = iy_N$ and

$$y_N = \frac{h}{(2hI/m + 1)^{1/2}}\,.$$

The force on the filament vanishes when $h = 0$ (lower branch) or (on the upper branch) when

$$h = 2m/I \tag{34a}$$

which gives a neutral point position

$$y_N = \frac{h}{\sqrt{5}}\,. \tag{34b}$$

The resulting flux (ψ_{ON}) and neutral point electric field (E_N) are given by Equations (31) and (32).

It is of interest for our later discussion to note that (33) may be deduced from the general form

$$B_y + iB_x = \frac{A(z - z_N^2)}{(z^2 + h^2)z^2}$$

with the three conditions that determine A, z_n, h being the behaviour at 0 ($\sim im/z^2$), the behaviour at ih ($\sim I/(z - ih)$) and the filament equilibrium.

Furthermore, the magnetic energy present may be written

$$W_B = \frac{1}{2\mu}\int_0^{\infty}\int_{-\pi/2}^{\pi/2}\left\{\frac{4h^2I^2}{r_1^2r_2^2} + \frac{m^2}{r^4} + \frac{4hIm}{r_1^2r_2^2r^2}(r^2 - h^2\cos 2\theta)\right\} r\,dr\,d\theta\,,$$

where the three terms represent the energy of the current-image pair, the energy of the background field, and the mutual energy of the current-image pair in the background,

© Kluwer Academic Publishers • Provided by the NASA Astrophysics Data System

1990SoPh..126..319P

and r, θ are polar coordinates of a point P with respect to the origin and a vertical axis while

$$r_1 = (h^2 + r^2 - 2hr\cos\theta)^{1/2},$$

$$r_2 = (h^2 + r^2 + 2hr\cos\theta)^{1/2},$$

are the distances of P from the current I and its image. After some algebra this reduces to

$$W_B = \frac{\pi I^2}{2\mu}\left\{2\log\frac{h}{R_p} + \frac{mB_0}{I^2} + \frac{2m}{Ih}\right\}, \tag{35}$$

where $B_0 = m/R_0^2$ is a typical active region field strength and R_0 is the cut-off distance at the origin (roughly the same as the diple depth h_B). Here the first term is the energy of the current and its image found previously in Equation (8). It is positive, as is the second term, while the third term is positive when $Im > 0$ but negative when $Im < 0$. When I and R_P are constant, W_B increases indefinitely with h, as before.

3.3. Effect of Gravity – Extra Solutions with Normal Polarity

When the force of gravity (Mg) is important, the equation of motion (27) becomes modified to

$$\frac{\mathrm{d}}{\mathrm{d}t}\left(M\frac{\mathrm{d}h}{\mathrm{d}t}\right) = \frac{2\pi I}{\mu}\left(\frac{I}{2h} - \frac{m}{h^2}\right) - Mg, \tag{36}$$

in the limit when $h \gg h_b$. When Mg is constant, the equilibria are, therefore, given by

$$\frac{hI}{m} = \frac{1 \pm (1 - 8G)^{1/2}}{2G}, \tag{37}$$

where $G = \mu Mgm/(\pi I^3)$ or

$$h = \frac{1}{2G_0}(1 \pm (1 - 8mG_0/I)^{1/2}), \tag{38}$$

where $G_0 = \mu Mg/(\pi I^2)$.

From (37) we can see that there are no equilibria when $G > \frac{1}{8}$ and two equilibria when $G < \frac{1}{8}$, being approximately $1/G$ and 2 when $G \ll 1$ (Figure 6(a)). Furthermore, the variation of the equilibrium height with dipole moment m from (38) is shown in Figure 6(b), which reveals several interesting features. (When the limit $h \ll h_b$ is not taken, a third solution with $h \approx h_b$ appears and bends back as in Figure 4.)

G_0 is a positive constant, and so when m and I have the same sign there are two solutions. These represent prominences with inverse polarity (Priest, 1989) in the sense that the magnetic field below the flux tube axis is oppositely directed from that near the photosphere (Figure 3(a)). We have, therefore, the effect of gravity on the solutions of

© Kluwer Academic Publishers • Provided by the NASA Astrophysics Data System

1990SoPh..126..319P

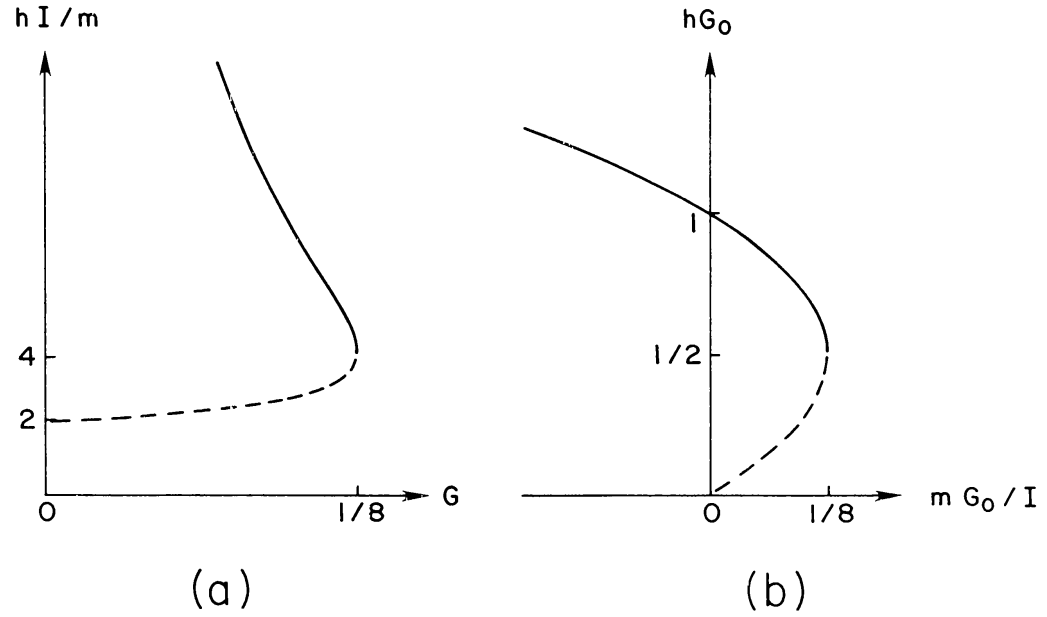

Fig. 6. (a) The equilibrium prominence height (h) as a function of $G = \mu Mgm/(\pi I^3)$. (b) The variation of the prominence height (h) with mG_0/I.

Sections 3.1 and 3.2, in which the curve in Figure 6(b) may be regarded as the continuation of the upper branch in Figure 4(a). Here the force $\pi I^2/(\mu h)$ of repulsion from the image is upwards, while gravity and the background force $2\pi Im/\mu h^2$) act downwards. Gravity paradoxically makes the equilibrium height of the lower branch increase above the value (34). It also in (36) has the effect of decreasing the acceleration at a particular height.

When m and I have opposite signs there is only one solution but it has a higher altitude $h \geq 1/G_0$ and a normal polarity, i.e., the same below the tube axis as the underlying photosphere (Figure 3(b)). It needs gravity to exist since the background force now acts upwards to reinforce the line-tying force and so gravity is the only force pulling downwards.

If g and M do not vary with height, the lower branch (dashed) in Figure 6(b) is unstable, but the upper branch and the normal polarity branch are stabilised by gravity, since an increase from the equilibrium heights keeps the downwards force of gravity the same in (36) but decreases the magnetic forces. Indeed the frequency (ω) of oscillation about the equilibrium is given by

$$\omega^2 = \frac{\mu Mh^2}{\pi I^2}(2G_0h - 1)\,. \tag{39}$$

Also to the right of the equilibrium curve in Figure 6(b), gravity dominates and makes the net force downwards. However, an unstable upper and normal polarity branch and, therefore, a flux tube eruption may occur if gravity decreases sufficiently fast with height (for high prominences) or if the prominence mass decreases with height (due to material draining out of a prominence as it moves upwards).

© Kluwer Academic Publishers • Provided by the NASA Astrophysics Data System

1990SoPh..126..319P

Alternatively, for a prominence of inverse polarity an eruption may be initiated by non-equilibrium near point P in Figure 4(a) with gravity being insufficient to stop the eruption as the prominence passes the upper branch. Thus, when the effect of gravity fall-off with height is included, the equation of motion (27) becomes

$$\frac{\mathrm{d}}{\mathrm{d}t}\left(M\frac{\mathrm{d}h}{\mathrm{d}t}\right) = \frac{2\pi I}{\mu}\left(\frac{I}{2h} - \frac{m}{(h+h_b)^2}\right) - \frac{Mg_0}{(1+h/R_0)^2} \,. \tag{40}$$

The equilibria now depend on the parameters $m/(h_b I)$, h_b/R_0, and $MgR_0/(\mu I^2)$, where R_0 is the solar radius. The potential energy becomes

$$W = -\frac{2\pi I}{\mu}\left(\frac{1}{2}\log\frac{h}{h_0} + \frac{m(h_0-h)}{(h+h_b)(h_0+h_b)}\right) + \\ + Mg_0\left(\frac{h-h_0}{(1+h/R_0)(1+h_0/R_0)}\right) .$$

For small values of $Mg_0h_b/(\mu I^2)$, the equilibrium (h_0 say) at low heights ceases to exist and produces an eruption starting from $h_0 \approx h_b$ and $W \approx 0$ when the value $m/(h_b I) = 2$ is exceeded. Using this critical value the potential energy becomes roughly

$$W = \frac{\pi I^2}{\mu}\left(-\log\frac{h}{h_b} + \frac{2(h-h_b)}{h+h_b}\right) + \frac{Mg_0(h-h_b)}{(1+h/R_0)(1+h_b/R_0)} \,. \tag{41}$$

The sum of the first two terms decreases from zero with height, whereas the last term increases from zero to $Mg_0R_0/(1+h_b/R_0)$ over distances of order R_0. Thus the effect of gravity is unable to stop the eruption if W remains negative, i.e., if for small values of h_b/R_0,

$$\frac{MgR_0}{I^2\mu} < \pi\log\frac{R_0}{h_b} \,. \tag{42}$$

It can be seen that gravity then has the effect of slowing the speed of rise below the value given in (31). Another effect which can slow the rise is the loss of energy via waves to the surrounding medium, which may be incorporated by including a term of the form $-v\,\mathrm{d}h/\mathrm{d}t$ on the right-hand side of Equation (40).

3.4. Constant prominence magnetic flux

For the magnetic field (25) representing the field of a prominence in a dipole background, the equilibrium when gravity is negligible is given from (27) by

$$\frac{I}{2h} = \frac{m}{(h+h_b)^2} \,. \tag{43}$$

© Kluwer Academic Publishers • Provided by the NASA Astrophysics Data System

1990SoPh..126..319P

The net magnetic flux below the prominence is

$$\psi_O = \int_0^{h-R_P} B_x(0,y)\,\mathrm{d}y = I \log \frac{2h - R_P}{R_P} - \frac{m}{h_b} \frac{(h - R_P)}{(h + h_0 - R_P)} . \tag{44}$$

Also, if the field in the prominence increases linearly at the flux tube axis to B_P at the lower boundary, the flux in the prominence is

$$\psi_P = \tfrac{1}{2} R_P B_P , \tag{45}$$

where

$$B_P = \frac{I}{R_P} + \frac{I}{2h - R_P} - \frac{m}{(h - R_P + h_b)^2} .$$

If the fluxes ψ_O and ψ_P remain constant (43)–(45) determine h, I, and R_P and in the limit when $h \gg R_P$, they reduce to the forms previously calculated in (12). Thus there are no new equilibria possible after the eruption and the rise speed is given from integrating (27) by

$$v^2 = \frac{2\pi I^2}{\mu M} \log \frac{h}{h_0} - \frac{4\pi I m}{M\mu} \frac{(h - h_0)}{(h + h_b)(h_0 + h_b)}$$

which increases indefinitely with h.

At the same time, since $I\,(= I_0)$ and R_P/h remain constant $(= R_{PO}/h_0)$, the magnetic energy (35) becomes,

$$W_B = \frac{\pi I_0^2}{2\mu} \left\{ 2 \log \frac{h_0}{R_{PO}} + \frac{m B_0}{I_0^2} + \frac{2m}{I_0 h} \right\} ,$$

so that only the last term varies with h, and in fact approaches zero as $h \to \infty$. This means that the magnetic energy difference between the initial and final state is

$$W_B^* = \frac{\pi I_0 m}{\mu h_0} , \tag{46}$$

where h_0 is the initial flux tube height.

Furthermore, the electric field at the neutral point from (32a) is

$$E_N = -\left(1 + \frac{2hI}{m}\right)^{-1/2} v ,$$

where $v = \mathrm{d}h/\mathrm{d}t$.

© Kluwer Academic Publishers • Provided by the NASA Astrophysics Data System

1990SoPh..126..319P

3.5. Constant magnetic twist

Suppose the prominence twist remains constant with the filament current decreasing with altitude like

$$I = \frac{I_0 h_0}{h} \tag{47}$$

and with the flux tube radius determined by (44) from flux conservation. If an equilibrium height (h_0) and current (I_0) are determined by (28) then the equation of motion (27) integrates to give (for $h \gg R_P$ and $h \sim h_b$) the subsequent kinetic energy as

$$\begin{aligned}\frac{1}{2}Mv^2 &= \frac{2\pi}{\mu}\int_{h_0}^{h}\left(\frac{I^2}{2h} - \frac{Im}{(h+h_b)^2}\right)\mathrm{d}h = \\ &= \frac{1}{2}\,\frac{\pi I_0^2 h_0^2}{\mu}\left(\frac{1}{h_0^2} - \frac{1}{h^2}\right) - \frac{\pi I_0 h_0 m}{\mu h_b^2} \times \\ &\quad \times \left(\log\frac{h(h_0+h_b)}{(h+h_b)h_0} + \frac{h_b(h_0-h)}{(h+h_b)(h_0+h_b)}\right)\end{aligned} \tag{48}$$

so that the rise speed increases more slowly than in the absence of the background field (Figure 5) and to a lower value, namely

$$v^2 \sim \frac{\pi I_0^2}{\mu M}\left(1 - \frac{2h_0 m}{I_0 h_b^2}\left[\log\left(1 + \frac{h_b}{h_0}\right) - \frac{1}{1 + h_b/h_0}\right]\right).$$

Furthermore, if damping of various kinds dissipates this energy, there is the possibility of a new equilibrium satisfying (43) and (47), namely

$$h = \frac{h_b}{\sqrt{(2m/I_0 h_0)} - 1}, \qquad I = \frac{I_0 h_0}{h_b}\left(\sqrt{\frac{2m}{I_0 h_0}} - 1\right),$$

which has $h > h_b$ provided $2m/(I_0 h_0) > 1$ or $h_0/h_b < 2m(I_0 h_b)$, which is always the case for initial equilibria given by (28).

In the limit $h \gg R_P$, $I \log h/R_P$ is constant ($= \psi_{OP}$) and the magnetic energy (35) becomes

$$W_B = \frac{\pi I_0 h_0}{2\mu}\left\{\frac{2\psi_{OP}}{h} + \frac{mB_0}{I_0 h_0} + \frac{2m}{h^2}\right\}$$

in which the first and third terms tend to zero as h increases to infinity, leaving only the energy of the background field. This implies that difference in magnetic energy between

© Kluwer Academic Publishers • Provided by the NASA Astrophysics Data System

1990SoPh..126..319P

the initial and final states is

$$W_B^* = \frac{\pi I_0}{\mu}\left\{\psi_O + \frac{m}{h_0}\right\}. \tag{49}$$

The flux up to the neutral point when $h_b I/m \ll 1$ and $h_b \ll y_N$ (Equation (31)) becomes

$$\psi_{ON} = \frac{I_0 h}{h}\log\frac{(1 + 2h_0 I_0/m)^{1/2} + 1}{(1 + 2h_0 I_0/m) - 1} - \frac{m}{h_b},$$

while the electric field (E_N) at the neutral point (Equation (32a)) reduces to

$$E_N = \frac{\mathrm{d}I}{\mathrm{d}t}\log\frac{(1 + 2h_0 I_0/m) + 1}{(1 + 2h_0 I/m) - 1},$$

where $\mathrm{d}I/\mathrm{d}t = -(I_0 h_0/h^2)v$ and $v = \mathrm{d}h/\mathrm{d}t$, so that E_N increases in magnitude with v.

3.6. Prominence as a current sheet

If the prominence is modelled as a current sheet stretching vertically on the y-axis from $y = H_1 = h - l/2$ to $y = H_2 = h + l/2$ and with a current density of $\mu j(h')/2\pi$, the flux function is

$$A = -\int_{H_1}^{H_2} j(h')\log\frac{z - ih}{z + ih}\,\mathrm{d}h' + \frac{im}{z + ih_b} \tag{50}$$

and the magnetic field is

$$B_y + iB_x = \int_{H_1}^{H_2}\frac{j(h')}{z - ih'} - \frac{j(h')}{z + ih'}\,\mathrm{d}h' + \frac{im}{(z + ih_b)^2}. \tag{51}$$

The global equilibrium height h may be calculated from (43) where $\mu I/2\pi$ is the total current in the prominence sheet, while I and l can be found from (50) by flux conservation in and below the sheet. In general the function $j(h')$ is given by the local internal prominence equilibrium, but a form such as

$$j(h') = (H_2 - h')^{1/2}(h' - H_1)^{1/2}$$

may be adopted to ensure that **B** is well-behaved near the ends of the prominence sheet. However, this is not easy to evaluate and so for simplicity the global behaviour may be estimated by setting $j(h')$ constant ($= I/l$). Then the flux below the prominence is (for $h \gg l$)

$$\psi_O = I\left(1 + \log\frac{2h}{l}\right) + \frac{m}{h + h_b}. \tag{52}$$

© Kluwer Academic Publishers • Provided by the NASA Astrophysics Data System

1990SoPh..126..319P

For constant ψ_O, this determines the way I decreases with h, more rapidly than in the absence of the background field (Equation (22)), and becoming zero when $h + h_b = m/\psi_O$. The resulting flux ψ_{ON} and field E_N are given by (31) and (32a), respectively.

The rise speed (v) then follows from the energy equation

$$\frac{1}{2}Mv^2 = \frac{\pi}{\mu}\int_{h_0}^{h}\left(\frac{I^2}{h} - \frac{2Im}{(h+h_b)^2}\right)\mathrm{d}h, \tag{53}$$

with the sheet height (l) determined by conservation of flux in the prominence, namely

$$\psi_P = -\frac{ml}{(h + l/2 + h_b)(h - l/2 + h_b)} \approx -\frac{ml}{(h+h_b)^2}, \tag{54}$$

in which the self-current I provides no net contribution. This shows that the prominence height (l) increases with altitude (h) like $(h + h_b)^2$.

The possibility of new equilibria in addition to an initial one (I_0, h_0, l_0) given by (43) may be estimated by solving (43) for I together with (52) and (54) for h and l in the forms

$$\frac{2h}{(h+h_b)^2}\left(1 + \log\frac{2h}{l}\right) + \frac{1}{h+h_b} = \frac{2h_0}{(h_0+h_b)^2}\left(1 + \log\frac{2h_0}{l_0}\right) + \frac{1}{h_0+h_b} \tag{55}$$

and

$$\frac{l}{(h+h_b)^2} = \frac{l_0}{(h_0+h_b)^2}. \tag{56}$$

4. Current Sheet Formation

In general for Inverse Polarity solutions, as the prominence rises due to nonequilibrium or instability, a current sheet may form about the X-point below the prominence. In Section 3 the effect of such a sheet has been neglected, but during the reconnection process a sheet must be present (Priest, 1985). When the reconnection is fast, the sheet is small but it may have a complex structure, the central sheet bifurcating into pairs of standing current sheets known as slow-mode shock waves which accelerate fast plasma jets. Also the jets may be slowed down by current concentrations (fast-mode shocks) as they encounter the ambient medium (Forbes and Priest, 1982; Biskamp, 1982). In addition the central sheet may itself break up into a series of current filaments as the reconnection becomes impulsive and bursty (Priest, 1985). When the reconnection is slow or in a flux pile-up regime (Priest and Forbes, 1986) or is inhibited for some reason, the current sheet may become much longer and have a greater influence on the global evolution.

© Kluwer Academic Publishers • Provided by the NASA Astrophysics Data System

1990SoPh..126..319P

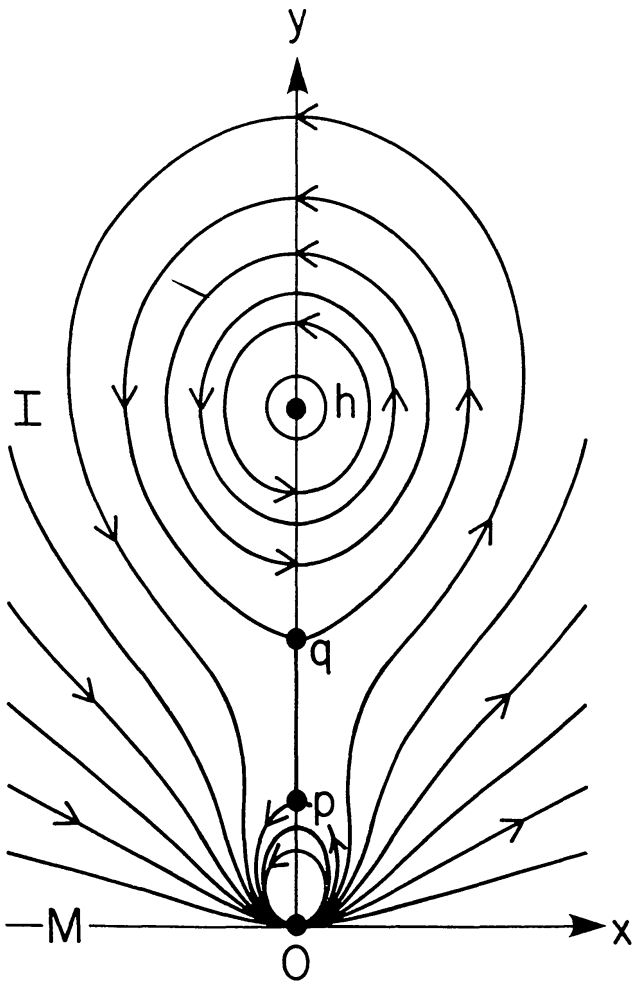

Fig. 7. Magnetic field lines for the low-β, MHD solution of a non-equilibrium case (p/h = 0.25 and q/h = 0.53).

4.1. General theory

The analysis of Section 3 refers to vacuum reconnection when there is no feedback of the plasma on the magnetic behaviour. It is a good approximation when the current sheet is small enough. Here we take account of a simple sheet of density $j(h')$ stretching from, say, P to Q at heights p and q above the solar surface (Figure 7). The magnetic field (25) is then modified to

$$B_y + iB_x = \frac{2ihl}{z^2 + h^2} + \frac{im}{(z + ih_b)^2} + \int_p^q \frac{2j(h')h'}{z^2 + h'^2}\,\mathrm{d}h' \quad . \tag{57}$$

Thus, except close to the current sheet, the effect of the sheet on the global field is negligible when its net current

$$J = \int_p^q j(h')\,\mathrm{d}h'$$

© Kluwer Academic Publishers • Provided by the NASA Astrophysics Data System

1990SoPh..126..319P

is much smaller than the prominence current.

In general $j(h')$ is determined by local prominence equilibrium but, as in Section 3.6, the global behaviour may be estimated by setting $j(h') = J/L$, where $L = q - p$ is the sheet length. Then the flux below the current sheet is

$$\psi_{OP} = I \log \frac{h+p}{h-p} + \frac{mp}{(p+h_b)h_b} + J\left(1 + \log \frac{2p}{L}\right) \tag{58}$$

for $p \gg L$. The field (57) becomes

$$B_y + iB_x = \frac{2ihl}{z^2+h^2} + \frac{im}{(z+ih_b)^2} + \frac{2ipJ}{z^2+p^2} \tag{59}$$

and so, when the sheet current (J) is so small that $pJ/(hl) \ll 1$ its effect is negligible.

Now from the imaginary part of (59) the field and its vertical gradient on the y-axis are

$$B_x = \frac{2hI}{h^2-y^2} - \frac{m}{(y+h_b)^2} + \frac{2pJ}{p^2-y^2} \tag{60}$$

and

$$\frac{\partial B_x}{\partial y} = +\frac{4hIy}{(h^2-y^2)^2} - \frac{2m}{(y+h_b)^3} + \frac{4pJy}{(p^2-y^2)^2} \,. \tag{61}$$

Setting these equal to zero at the midpoint ($y = p + L/2$) of the sheet (cf. Kaastra, 1985; Martens, 1986) gives in the limit $p \gg L$

$$\frac{2hI}{h^2-p^2} - \frac{m}{(p+h_b)^2} - \frac{2J}{L} = 0 \,, \tag{62}$$

$$\frac{2hIp}{(h^2-p^2)^2} - \frac{m}{(p+h_b)^3} - \frac{2J}{L^2} = 0 \,. \tag{63}$$

These two equations together with (58) may be used to determine the current sheet properties (J, L, p) once ψ_{OP}, h, and I are known. At one extreme we have vacuum reconnection with $\psi_{OP} = \psi_{ON}(t)$, $J = 0$, $L = 0$, $p = y_N$ and at the other extreme no reconnection is allowed and ψ_{OP} remains constant, equal to the initial flux ($\psi_{ON}(0)$) up to the neutral point at the onset of the eruption. In general, however, the reconnected flux $\psi_{OP} - \psi_{ON}(0)$ may lie between the vacuum value and zero.

The vertical equation of motion (27) of the prominence becomes modified to

$$\frac{\mathrm{d}}{\mathrm{d}t}\left(M\frac{\mathrm{d}h}{\mathrm{d}t}\right) = \frac{2\pi I}{\mu}\left(\frac{I}{2h} - \frac{m}{(h+h_b)^2} - \frac{2pJ}{h^2-p^2}\right) \tag{64}$$

© Kluwer Academic Publishers • Provided by the NASA Astrophysics Data System

1990SoPh..126..319P

and so the current sheet exerts an extra downwards force on the prominence, tending to slow it down by comparison with the vacuum case. Integrating yields the prominence kinetic energy

$$\frac{1}{2}Mv^2 = \frac{\pi}{\mu}\int_{h_0}^{h}\left(\frac{I^2}{h} - \frac{2Im}{(h+h_b)^2} - \frac{4pIJ}{h^2-p^2}\right)\mathrm{d}h\,. \tag{65}$$

Also from (60) the net magnetic flux below the prominence is modified from (44) to

$$\psi_O = I\log\frac{2h-R_P}{R_P} - \frac{m(h-R_P)}{h_b(h+h_b-R_P)} + J\log\frac{h-R_P+p}{h-R_P-p}\,. \tag{66}$$

Following Section 3.4 the flux in the prominence is now

$$\psi_P = \frac{1}{2}R_P\left\{\frac{2hI}{R_P(2h-R_P)} - \frac{m}{(h-R_P+h_b)^2} + \frac{2pJ}{p^2-(h-R_P)^2}\right\} \tag{67}$$

and so, if ψ_O and ψ_P remain constant, (64), (66), (67) determine h, I, and R_P as functions of time (Figure 8(a)).

If instead ψ_O and the prominence twist remains constant with

$$I = \frac{I_0 h_0}{h}\,, \tag{68}$$

then (64), (66), (68) determine the way h, I, and R_p vary (Figure 8(b)).

4.2. A PARTICULAR SELF-CONSISTENT SOLUTION

In the limit of zero plasma beta, currents in two-dimensional, ideal MHD become concentrated at singularities and branch cuts in the complex plane. To model an erupting current filament with a current sheet below it we may choose a solution of the form

$$B_y + iB_x = \frac{iA(z^2+p^2)^{1/2}(z^2+q^2)^{1/2}}{z^2(z^2+h^2)} \tag{69}$$

which incorporates a line current at $z = ih$, an image line current at $z = -ih$, a two-dimensional dipole field at $z = 0$, and a current sheet stretching from $z = ip$ to $z = iq$ as shown in Figure 7.

The three parameters A, p, and q are not arbitrary, but are instead fixed by the following ideal-MHD constraints.

(i) Near $z = ih$ the field should behave like $I/(z - ih)$, where I may be a function of h.

(ii) Near $z = 0$ the field should behave like im/z^2, where m is constant.

© Kluwer Academic Publishers • Provided by the NASA Astrophysics Data System

1990SoPh..126..319P

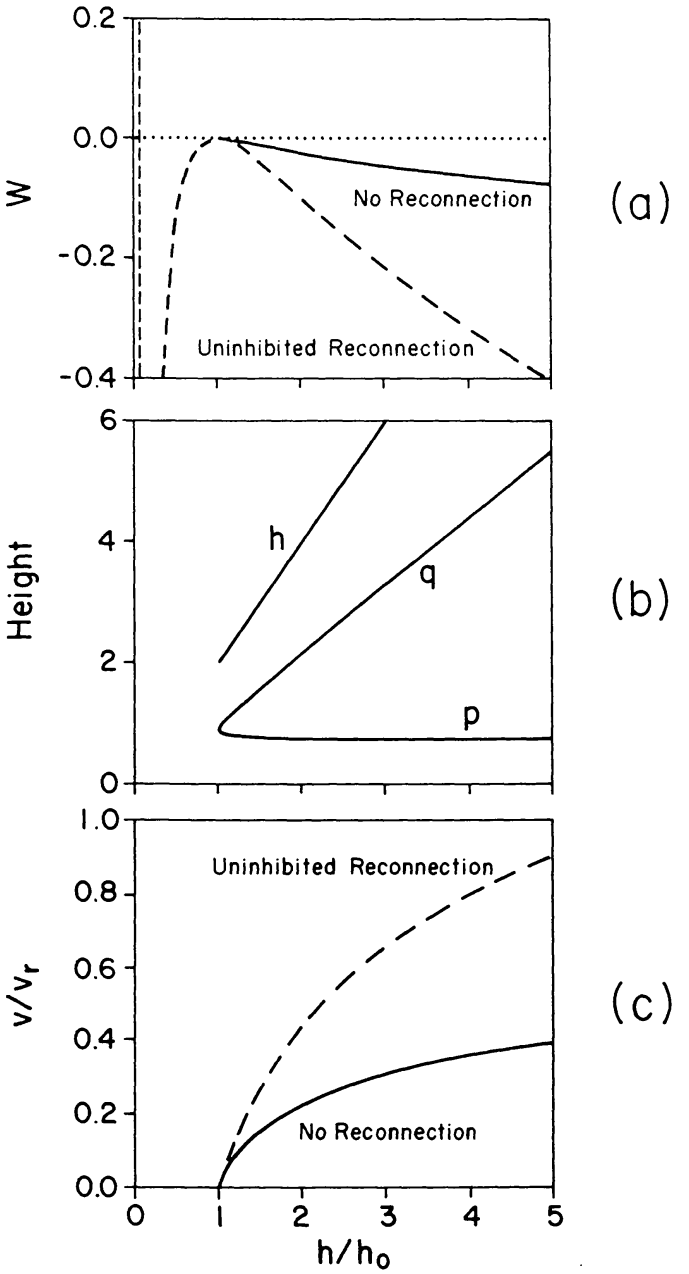

Fig. 8. (a) The magnetic work W (in units of $\pi I^2/\mu$) of the self-consistent, MHD solution for $h > 2$ (solid curve) and the vacuum solution for $h_b = 0$ (dashed curve) as a function of filament height h (in units of $y_N = h_0/\sqrt{5}$, the X-line height when there is no current sheet). (b) The corresponding upper and lower edges of the current sheet (q and p, respectively) as functions of height h. (c) The corresponding velocity as a function of height.

(iii) The magnetic flux between the dipole at $z = 0$ and the bottom edge of the current sheet at p should be constant.

(iv) The magnetic flux between the filament at $z = ih$ and the top edge of the current sheet at q should also be constant.

The form (69) represents a generalization of the field of Section 3.2 to include a current sheet of finite length, and it has the same property that the normal photospheric field (along $z = x$) is constant in time and independent of h, q, and p (i.e., the magnetic field is line-tied at the photosphere).

© Kluwer Academic Publishers • Provided by the NASA Astrophysics Data System

1990SoPh..126..319P

Applying conditions (i) and (ii) at $z = ih$ and 0 gives

$$A = mh^2/pq \tag{70}$$

and

$$\frac{2hpq}{(h^2 - p^2)^{1/2}(h^2 - q^2)^{1/2}} = \frac{m}{I}\,, \tag{71}$$

where I is a yet-to-be-determined function of h. The flux condition (iii) gives

$$\int_0^p f(y)\,\mathrm{d}y = \psi_{OP}\,, \tag{72}$$

where

$$f(y) = \frac{mh^2(p^2 - y^2)^{1/2}(q^2 - y^2)^{1/2}}{pqy^2(y^2 - h^2)}$$

is the magnetic field along the y-axis.

If the initial state is of the form (33), then we have

$$\psi_{OP} = \int_0^{y_N} f_0(y)\,\mathrm{d}y\,, \tag{73}$$

where

$$f_0(y) = \frac{2h_0I_0}{h_0^2 - y^2} - \frac{m}{y^2}\,,$$

in terms of the initial filament current (I_0), filament height (h_0) and neutral line height (y_N). The integrals (72) and (73) are infinite due to the singularity of the diple field at $z = 0$. This singularity can be removed without affecting the flux constraint (iii) since the dipole field is independent of h and, hence, constant. Subtracting the dipole contribution between $z = 0$ and $z = iy_N$ from both sides of (72) gives

$$\int_0^p f(y) + \frac{m}{y^2}\,\mathrm{d}y = \int_0^{y_N} \frac{2h_0I_0}{h_0^2 - y^2}\,\mathrm{d}y + \int_{y_N}^p \frac{m}{y^2}\,\mathrm{d}y$$

or equivalently,

$$\frac{h_0}{2}\int_0^p \frac{1}{y^2}\left(-\frac{h^2(p^2 - y^2)^{1/2}(q^2 - y^2)^{1/2}}{(h^2 - y^2)pq} + 1\right)\mathrm{d}y =$$

$$= \log\frac{\sqrt{5} + 1}{\sqrt{5} - 1} + \frac{\sqrt{5}\,p - h_0}{2p}\,. \tag{74}$$

© Kluwer Academic Publishers • Provided by the NASA Astrophysics Data System

1990SoPh..126..319P

In deriving (74) we have used the expressions $h_0 = 2m/I_0$ and $y_N = h_0/\sqrt{5}$ from Equation (34).

So far, we have applied conditions (i) through (iii) to determine the parameters A, p, and q, but these three parameters are not yet fully specified since they depend on $I(h)$ which remains undetermined at this point. To determine $I(h)$ we use the last condition (iv) which requires that the flux between the top of the current sheet (q) and the filament (h) be constant.

Recall that in Sections 2.1 and 2.2 we found for the vacuum case with no current sheet that the filament current cannot be kept constant unless there is an external source to pump energy into the system. If no such external source exists, then the current in the vacuum case decreases as

$$I = I_0 \frac{\log[(2h_0/R_P) - 1]}{\log[(2h/R_P) - 1]} ,$$

where the filament radius R_P is constant. In the limit that R_P equals zero, $I = I_0$, and the current no longer increases as h increases, provided h approaches infinity more slowly than R_p approaches zero. However, if h approaches infinity more rapidly than R_P approaches zero, the current I at infinity can approach zero rather than I_0.

For the self-consistent solution of this section we have already taken the limit R_P equals zero in obtaining condition (iv), so one expects that, as in the vacuum case, $I = I_0$ in this limit. To show this explicitly we follow the same procedure that we used at the base to obtain (74) from the flux conservation condition (ii). The magnetic flux from the top of the current sheet to the filament is

$$\psi_{qh} = \int_q^h f(y)\,dy , \tag{75}$$

where

$$f(y) = \frac{mh^2(p^2 - y^2)^{1/2}(q^2 - y^2)^{1/2}}{pqy^2(y^2 - h^2)} .$$

As before, the integral (75) is infinite, but this time the infinite value is due to the singularity at $y = h$ instead of the one at $y = 0$. We can remove the singularity at $y = h$ by subtracting the initial filament field between y_N and h from both sides,

$$\int_q^h f(y) + \frac{I_0}{y - h}\,dy = \int_{y_N}^{h_0} \frac{I_0}{y + h_0} - \frac{m}{y^2}\,dy + \int_q^{h-(h_0-y_N)} \frac{I_0\,dy}{y - h} ,$$

or equivalently when $I = I_0$,

© Kluwer Academic Publishers • Provided by the NASA Astrophysics Data System

1990SoPh..126..319P

$$\int_q^h \frac{1}{y-h}\left(1 - \frac{h_0 h^2 (y^2-p^2)^{1/2}(y^2-q^2)^{1/2}}{2pqy^2(y+h)}\right) dy =$$

$$= \log \frac{(\sqrt{5}-1)2h_0}{(\sqrt{5}+1)(h-q)} - \frac{1}{2}(\sqrt{5}-1)\,. \tag{76}$$

At $y = h$ the integrand of the integral in (76) reduces to

$$\lim_{y\to h} \frac{I_0 - I}{y-h}\,, \tag{77}$$

when (71) is used to eliminate m. Now if $I \neq I_0$, (77) is infinite, and the corresponding integral in (76) is also infinite. Thus, for $I \neq I_0$ there is no solution which satisfies (76).

For $I = I_0$, the value of the integral in (76) can be found by taking limits. We do this by letting

$$I = I_0(1-\delta)$$

and rewriting (76) as

$$g(h) + \lim_{R_p\to 0} \delta \int_q^{h-R_p} \frac{dy}{y-h} = \log \frac{2\sqrt{5}}{1+\sqrt{5}} + \frac{1-\sqrt{5}}{2} = -0.2945\,, \tag{78}$$

where

$$g(h) = \int_q^h \frac{1}{y-h}\left(\frac{h_0 h^2 (y^2-p^2)^{1/2}(y^2-q^2)^{1/2}}{2pqy^2(y+h)} - 1\right) dy -$$

$$- \log \frac{2(\sqrt{5}-1)h_0}{\sqrt{5}\,(h-q)}\,.$$

Evaluation of the integral in (78) gives

$$g(h) + \lim_{R_p\to 0} \delta \log \frac{h-q}{R_p} = -0.2945\,. \tag{79}$$

Unlike the integral in (76), $g(h)$ can easily be evaluated using L'Hôpital's rule. Table I lists numerically determined values of g, p, and q as functions of h, where q and p are determined by numerical integration of the lower flux constraint (74). (See also Figure 8(b).) The table shows that $g(h)$ is a slowly increasing function of h. Thus, to satisfy the upper flux constraint (79) we require that

$$\delta = -\lim_{R_p\to 0} \frac{g(h) + 0.2945}{\log[(h-q)/R_p]} = 0\,. \tag{80}$$

© Kluwer Academic Publishers • Provided by the NASA Astrophysics Data System

1990SoPh..126..319P

TABLE I

Numerically derived values of $g(h)$

h	p	q	g
2.0	0.894	0.894	−0.294
2.1	0.834	1.012	−0.257
2.2	0.816	1.088	−0.219
2.3	0.805	1.156	−0.182
3.5	0.769	1.874	0.200
4.6	0.762	2.498	0.463

Note that although δ is zero, the term in which it occurs in (79) is not. Putting this term to zero corresponds to setting the filament current constant even when the filament radius R_P is finite, and when this is done, flux is not conserved between the filament and the upper edge of the current sheet. Just as in the vacuum case, the current in the filament must decrease as h is increased. However, as R_p approaches zero the amount of current decrease required becomes increasingly small because the amount of flux between the sheet and the filament is approaching infinity. Thus in the limit $R_p = 0$, only an infinitesimally small change in the filament current is required.

Filament equilibria occur when the external force on the filament is zero, i.e.,

$$\lim_{y \to h} \left[f(y) + \frac{I}{y - h} \right] = 0 . \tag{81}$$

In other words, after a little algebra,

$$\frac{mI[h^4 - 3(p^2 + q^2)h^2 + 5p^2q^2]}{4h^2pq(h^2 - p^2)^{1/2}(h^2 - q^2)^{1/2}} = 0 , \tag{82}$$

which has the two solutions

$$h^2 = \tfrac{1}{2}[3(p^2 + q^2) + \sqrt{9p^4 + 9q^4 - 2p^2q^2}] \tag{83}$$

and

$$h = \infty . \tag{84}$$

The first solution is unstable, while the second is stable. When the lower flux constraint (73) is applied one finds $p = q = y_N$, and (83) reduces to

$$h = \sqrt{5}\, y_N . \tag{85}$$

Thus, there are only two equilibria. The first has no current sheet and corresponds to the vacuum model configurations when $h_b = 0$. The second equilibrium has a semi-infinite current sheet which extends to $h = \infty$ from $h = p_\infty$, where

$$p_\infty = \frac{m\pi/I_0}{2 \ln[(\sqrt{5} + 1)/(\sqrt{5} - 1)] + \sqrt{5}} = 0.7550(m/I_0) . \tag{86}$$

© Kluwer Academic Publishers • Provided by the NASA Astrophysics Data System

1990SoPh..126..319P

Equation (86) is obtained by evaluating (74) in the limit that h and q are much larger than p.

The magnetic work and corresponding kinetic energy are obtained by numerically integrating the force on the filament over h. This force is simply I times the left-hand side of (82), and when integrated it gives the magnetic work and filament speed as shown in Figure 8. As in the vacuum model the magnetic energy of the system decreases as the filament moves upwards, but the magnetic energy release in the MHD case is only about 12% of the energy released in the vacuum case at any given h. The difference in energy is due to the formation of the current sheet.

5. Conclusion

We have modelled in Section 2 an erupting prominence as a horizontal twisted magnetic flux tube being repelled from the solar surface by magnetic pressure forces. Mathematically, this is treated by replacing the flux tube by a line current (I) and the repulsive force by the force from an image line current below the photosphere. The prominence height (h) and rise speed (v) are determined by the equation of motion, but one first needs an extra physical assumption to determine the current (I). Holding I constant by itself is found to increase the magnetic potential energy rather than decrease it as the prominence rises since the magnetic flux (ψ_O) below the prominence increases. Holding ψ_O constant instead means that one needs one more assumption to determine the prominence rises since the magnetic flux (ψ_O) below the prominence increases. Holding ψ_O constant instead means that one needs one more assumption to determine the prominence radius (R_P). For example, if R_P remains constant, then the current decreases logarithmically with height and the rise speed increases up to a constant value at large heights. Alternatively, if the azimuthal flux inside the prominence is held constant (as in the numerical experiment of Forbes, 1989), then R_P may increase linearly or, if R_P is constant, a surface current forms on the filament. A preferable assumption is to set the prominence twist constant, in which case the current decreases like h^{-1}, while the tube radius increases to a maximum and then declines towards zero and the speed increases up towards a constant value.

When the prominence itself is modelled as a vertical current sheet, its current falls off logarithmically with height when the flux below the prominence is fixed and the rise speed increases up to a constant value.

When a background magnetic field is incorporated with a dipole form having a depth h_b (Section 3), the initial equilibrium before the eruption of a prominence with Inverse Polarity can also be modelled. As the dipole moment (m) decreases or the flux tube twist or current increases, so the prominence passes slowly through a series of equilibria until, when (m/h_bI) becomes less than 2, there is no longer an equilibrium and the prominence erupts. If the prominence current or flux remains constant, the rise speed increases indefinitely, while the electric field (E_N) at the neutral point below the prominence increases to a maximum and then decreases towards zero at large heights. If the

© Kluwer Academic Publishers • Provided by the NASA Astrophysics Data System

1990SoPh..126..319P

prominence twist remains constant the prominence speed increases to a constant value, smaller than in the absence of the background field, while the reconnection electric field is proportional to the prominence speed.

The effect of gravity is also included, which is more important for quiescent prominences than for active-region prominences (where the magnetic field dominates). When m and I have the same sign there are two equilibrium solutions for prominences with Inverse Polarity and heights below $G_0 = \mu Mg/(\pi I^2)$ in which the repulsion from the image current acts upward while gravity and the background force act downwards. When m and I have opposite signs there is an equilibrium of normal polarity at a height larger than G_0 and with the background force now acting upwards. If gravity and the prominence mass (M) are constant the lower inverse polarity branch is unstable, while the upper inverse polarity branch and the normal polarity branch are stable, although eruption of a normal polarity prominence may occur if gravity decreases rapidly enough with height or if the prominence mass drains away as the prominence moves upward. Alternatively, an inverse polarity prominence may erupt by non-equilibrium as before when gravity is insufficient to stop the eruption as the prominence passes the upper branch.

Finally, a self-consistent ideal MHD solution is obtained in the low-β limit which describes the formation of a current sheet below an erupting filament. The solution shows that the formation of the current sheet does not prevent the ideal instability or non-equilibrium which drives the eruption. However, the formation of the sheet does reduce the energy released by the ideal process by about 90%. In practice reconnection at the sheet will be driven by the eruption (Steele and Priest, 1989) and so will release the extra energy.

Acknowledgements

The authors are grateful to the National Science Foundation (NSF grant ATM-8711089), the National Aeronautics and Space Administration (NAGW-76), and the UK Science and Engineering Research Council for financial support. ERP is also thankful to Joe Hollweg for warm hospitality during his summer visit to Durham.

References

Amari, T. and Aly, J. J.: 1989, *Astron. Astrophys.* **208**, 261.
Anzer, U.: 1989, in E. R. Priest (ed.), *Dynamics and Structure of Quiescent Solar Prominences*, Kluwer Academic Publishers, Dordrecht, The Netherlands, Ch. 6.
Biskamp, D. and Welter, H.: 1989, *Solar Phys.* **120**, 49.
Browning, P. K. and Priest, E. R.: 1986, *Solar Phys.* **106**, 335.
Demoulin, P. K. and Priest, E. R.: 1988, *Astron. Astrophys.* **206**, 336.
Demoulin, P. K. and Priest, E. R.: 1990, to be submitted.
Forbes, T. G.: 1986, *Astrophys. J.* **305**, 553.
Forbes, T. G.: 1990, to be submitted.
Forbes, T. G. and Priest, E. R.: 1983, *Solar Phys.* **88**, 211.
Hood, A. W. and Priest, E. R.: 1980, *Solar Phys.* **66**, 113.
Kaastra, J. S.: 1985, Ph.D. Thesis, Univ. Utrecht.

© Kluwer Academic Publishers • Provided by the NASA Astrophysics Data System

1990SoPh..126..319P

Kuin, N. and Martens, P.: 1986, in A. Poland (ed.), *Coronal and Prominence Plasmas*, NASA CP-2442, p. 241.
Kuperus, M. and Raadu, M. A.: 1974, *Astron. Astrophys.* **31**, 189.
Martens, P.: 1986, in A. Poland (ed.), *Coronal and Prominence Plasmas*, NASA CP-2442, p. 431.
Mikic, Z., Barnes, D. C., and Schnack, D. D.: 1988, *Astrophys. J.* **328**, 830.
Poletto, G. and Kopp, R. A.: 1986, in D. F. Neidig (ed.), *The Lower Atmosphere of Solar Flares*, NSO, Sacramento Peak, NM, p. 453.
Priest, E. R.: 1981, *Solar Flare MHD*, Gordon and Breach, London.
Priest, E. R.: 1982, *Solar MHD*, D. Reidel Publ. Co., Dordrecht, Holland.
Priest, E. R.: 1985, *Rep. Prog. Phys.* **48**, 955.
Priest, E. R.: 1986, in P. Gondhalekar (ed.), *Proc. RAL Workshop on Solar and Stellar Flares*, p. 140.
Priest, E. R.: 1989, *Dynamics and Structure of Quiescent Solar Prominences*, Kluwer Academic Press, The Netherlands.
Robertson, J. A. and Priest, E. R.: 1987, *Solar Phys.* **114**, 311.
Steele, C. D. and Priest, E. R.: 1989, *Solar Phys.* **119**. 157.
Sturrock, P.: 1980, *Solar Flares*, Colo. Ass. Univ. Press.
Van Tend, W. and Kuperus, M.: 1978, *Solar Phys.* **59**, 115.
Zwingmann, W.: 1985, Ph.D. Thesis, Bochum University.

© Kluwer Academic Publishers • Provided by the NASA Astrophysics Data System